International Journal of Thermofluids 26 (2025) 101089

Contents lists available at ScienceDirect

International Journal of Thermofluids

journal homepage: www.sciencedirect.com/journal/international-journal-of-thermofluids

Parametric analysis for thermally magnetized hybrid ternary (TMHT) nanofluid flow on thin film with temperature stratification

Tanuja T. N [a,b], Kavitha L [a], Khalil Ur Rehman [c,*], S.V.K Varma [a], Wasfi Shatanawi [c,d], G.V. Kumar [e], Zeeshan Asghar [c]

[a] Department of Mathematics, School of Applied Sciences, REVA University, Bengaluru, Karnataka, India
[b] Department of Mathematics, CHRIST (Deemed to be University), Bengaluru, India
[c] Department of Mathematics and Sciences, College of Humanities and Sciences, Prince Sultan University, Riyadh, 11586, Saudi Arabia
[d] Department of Mathematics, Faculty of Science, The Hashemite University, P.O. Box 330127, Zarqa, 13133, Jordan
[e] Department of Mathematics, CSSR & SRRM Degree & PG College, Kamalapuram 516289, A.P., India

ARTICLE INFO

Keywords:
Heat transfer
Temperature stratification
Ternary nanofluid
Stretched surface
Magnetic field

ABSTRACT

The thermophysical examination of flow field claims various applications in both scientific and industrial domains and hence it remains important to inspect especially when both the heat and mass transfer are taken simultaneously. Owning such motivation, the present study offers a response surface optimization for thermal flow field of hybrid ternary water-based aluminium, silicon and Zinc nanofluid over a stretched surface manifested with both temperature stratification and concentration stratification effects. The governing equations are formulated for mathematical model and those PDE's are reduced to ODE's by using appropriate similarity transformations. Those obtained resultant equations are solved numerically by using Runge Kutta Fehlberg fourth fifth-order (RKF 45) technique. The supremacy of essential aspects on the flow field, heat and mass transfer rates were analyzed using graphical representation. Additionally, Response surface Methodology is performed to derived the heat transfer rate as a response function for the input factors for different parameters. From the graph it is noticed that temperature profile drops as the thermal stratification parameter increases. The temperature admits the direct relation with an increase in the solid volume fraction of ternary nanofluids. From RSM it is noticed that adjusted R-squared and R-squared are obtained as 100 % accuracy of the mathematical model.

1. Introduction

The extrusion of plastic and rubber sheets, extrusion and coating, fiber spinning, aircraft wing and fuselage design and wind turbine blades and paper production are the practical applications of stretched surfaces. By considering such importance various studies were conducted by researchers to examine stretched surfaces like Crane [1] provided the ground-breaking work on the precise answer to a closed structure for fluid flow past a stretched sheet. Building on Crane's foundation, numerous researchers, including Gupta [2], Char and Chen [3], Dutta et al. [4], and Bhattacharyya et al. [5], have extended the work to encompass both Newtonian and non-Newtonian fluids, considering the influences of thermal and mass transference under assorted conditions. Tsou et al. [6] investigated fluid flow and heat transmission in the boundary layer on constantly moving surfaces. Bhukta et al. [7] explored the impact of thermal transmission and mass on an electrically conducting viscoelastic fluid flowing over a shrinking sheet in the presence of an energy source. The study provided an exact solution for the temperature field, and the applied magnetic field was found to enhance both velocity and concentration distributions. The utilization of nonlinear stretching sheets plays a significant role in various industrial applications, for example, in dye extrusion of polymer sheets and cooling baths used for drying metal plates. A nonlinear stretching sheet was studied by Das [8] for a fluid with partial slip. Fluid velocity decreased as mass diffusivity increased on surfaces with increasing partial slip and nonlinearity indices. Cortell [9] explored the impact of nonlinearity parameters and found that higher values increased skin friction, providing more resistance to fluid flow. This resistance resulted in a reduction in fluid stream velocity and an increase in thermal transmission.

The application of a Magnetic Field (MHD) to a stretching sheet is

* Corresponding author.
E-mail address: kurrehman@psu.edu.sa (K.U. Rehman).

https://doi.org/10.1016/j.ijft.2025.101089

Available online 16 January 2025

Nomenclature

U_w	velocity of surface (m/s)
$h(t)$	film thickness
T^*	temperature (K)
C^*	Concertation
S_t	thermal stratification
S_m	mass stratification
Nb	Brownian motion
Nt	thermophoresis motion
Sc	Schmidt number
Pr	Prandtl number
Ec	Eckert number
S	unsteadiness parameter
M	Magnetic field
C_{fx}	Skin friction co-efficient
$f(\eta)$	dimensionless stream function
Nu_x	Nusselt number
Sh_x	Sherwood number
u_1^*, u_2^*	velocity components (m/s)
D_B	Brownian diffusion coefficient(m^2/s)
D_T	Thermophoresis diffusion coefficient(m^2/s)
Re_x	Rayleigh number
T_w	Wall temperature
C_w	Surface concentration

Greek letters

β	Thermal expansion coefficient$(1/K)$
ϕ	Solid volume fraction of nanoparticles
α	Thermal diffusivity of base fluid(m^2/s)
η	dimensionless similarity variable
ψ	Stream function
$\theta(\eta)$	Dimensionless temperature
$\varphi(\eta)$	Dimensionless concentration

Subscript

f	base fluid
nf	nanofluid
hnf	hybrid nanofluid
tnf	ternary hybrid nanofluid

exemplified in the manufacturing of polymer sheets, where the final product's characteristics depend significantly on the rate of stretching raw materials. In the industrial context, numerous studies have explored fluid flow behavior on stretching and nonlinear stretching sheets. In a three-dimensional multi-harmonic heterogeneous (MHD) boundary layer with convective boundary conditions, Nadeem et al. [10] studied Casson nanofluid flow across a linearly stretched sheet. Casson nanofluid flow model on a nonlinearly stretched sheet was developed by Mustafa et al. [11] and includes the effects of magnetic fields. An investigation into the heat transmission of electromagnetic fluid across a stretched surface was carried out by Mutuku et al. [12] using a computer. A decrease in the temperature profile was noted when the thermal stratification parameter values increased, as they investigated the unsteady MHD boundary layer heat and mass transfer of nanofluid across a flat surface with double stratification. According to Mehmood et al. [13], the velocity profile of a viscous nanofluid across an inclined stretched sheet decreases as the thermal and mass stratification parameters increase. This flow is an unstable MHD boundary layer heat and mass transfer process.

Base fluids like oil, ethylene glycol, and water exhibit limited thermal conductance, posing challenges in fluid flow. To enhance thermal conductivity, scientists introduced techniques such as suspending small particles, pioneered by Choi and Eastman [14]. These nanofluids find industrial use for cooling in power plants, auto engines, technological gadgets, and production methods. Recent studies have focused on heat transmission, such as the work of Sheikholeslami and Ganji [15] on water-based copper nanofluid flow between squeezing plates. Authors employed Brinkman and Garnetts models to determine viscosity and thermal conductivity, concluding that thermal conductance is influenced by Eckert number and nanoparticle concentration. According to Hayat et al. [16], who investigated Burger nanofluid flow over a stretching sheet, higher thermophoresis and Brownian motion factors under Robin-type conditions support the thermal flow rate. Investigating the development of irreversibility in the flow system, Makinde and Eegunjobi [17] investigated the combined effects of a magnetic field, changing viscosity, thermophoresis, and Brownian motion on nanofluid. Nanofluid flow has been found to reduce heat transfer resistance in various flow systems [18–20]. Over time, researchers discovered that introducing various kinds of nanoparticles into a base fluid further enhances thermal flow characteristics, coining the term "hybrid nanofluid." Researchers Lund et al. [21] investigated the effects of heat radiations and viscous dissipation on the dynamics of hybrid nanofluid flows over a stretched surface. They identified two branches of solutions, noting that the upper branch, characterized by stability, proves more applicable by investigating different flow geometries and circumstances. Khan et al. [22–24] accomplished an outstanding study on improving thermal flow in a hybrid nanofluid. The phrase "trihybrid nanofluid" was coined from recent research showing that three distinct kinds of nanoparticles suspended in a pure fluid can optimize thermal conductivity. New formulae for Nusselt number estimate and thermophysical properties were introduced by Sundar et al. [25] for ternary hybrid nanofluid flow with GO, Fe3O4, and TiO2 nanoparticles in ethylene glycol. They determined that the flow system's thermal performance was 14.32 % better. Using trihybrid nanofluid and various nanoparticle morphologies, Sahoo [26] investigated thermal flow and irreversibility, finding an entropy rise of 12.24 % from 1 % to 3 % concentration growth. The heat flow properties of ternary hybrid nanofluids with convective heat transfer over a stretched sheet were shown to be superior to those of other hybrid or conventional nanofluids, according to research by Manjunatha et al. [27]. Heat transfer analysis with ternary nanofluid with the combination of Fe_2O_4 – ZnO – $CoFe_2O_4$ – H_2O across Riga plate considering Newtonian heating effect was investigated by Mahabaleshwar et al. [28]. Chemically dynamic magnetic hydrodynamic convective flow and heat transfer efficiency of a ternary blend of hybrid nanoparticles passing over a curved expanding surface was analyzed by Muhammad et al. [29]. Azeem et al. [30] investigated the dynamics of flow and thermal exchange within a slender layer of Cu-nanofluid on an elongated surface, incorporating various geometric factors (platelets, blades, bricks, spheres, and cylinders) alongside slip and convective constraints. It is observed that among the array of particle shapes, the Platelet-like nanoparticles exhibit the most efficient heat transfer capability compared to their counterparts.

Stratification, influenced by temperature or concentration variations, significantly impacts heat and mass transfer rates. Researchers are paying close attention to the phenomenon of double stratification, which happens when mass and heat transport processes occur simultaneously, because of its importance in many technical and industrial contexts. Thermal stratification, for instance in reservoirs, plays a crucial role in affecting oxygen levels through biological processes. Heat rejection in natural settings, thermal energy storage in systems like solar ponds, industrial food products and atmospheric heterogeneous mixtures are some of the applications. The investigation of thermal stratification is particularly essential in solar engineering, as effective

stratification contributes to higher energy efficiency. Due to its significance in engineering and industrial processes, researchers including Srinivasachary and Upendar [32], Ibrahim and Mankinde [31], and Srinivasacharya and Surender [33] have investigated the effects of double stratification on heat transmission and flow characteristics. Srinivasacharya and Surender [34] found that when thermal stratification increases, the rates of heat, mass, and nanoparticle transfer decrease in a mixed convection investigation involving a porous medium saturated with nanofluids and a vertical plate.

The combined effects of chemical reactions and double stratification on the mass and heat transfer properties of nanofluid flow over a porous stretched sheet were investigated by Sudarsana & Sreedevi [35]. Thermal radiation adds another layer of intricacy to the system. The impact of double stratification on nanofluid unstable electrical MHD mixed convection flow, taking viscous dissipation and Joule heating into account, is investigated by Daniel et al. [36].

Ying et al. [37] studied the effects of thermal diffusivity and melting phenomenon in Carreau nanofluid flow restricted by nonlinear stretching cylinder with convective Marangoni boundary constraints. Ying et al. [38] examined the impact of unsteady mixed convection flow of magneto-Williamson nanofluid due to stretched cylinder with significant non-uniform heat source/sink features. Cao et al. [39] Comparatively study the ternary-hybrid nanofluid flows caused by forced convection, free convection, and mixed convection where radiative heat flux is heavily influenced by temperature difference, as in non-linear thermal radiation, and partial slip. Cao et al. [40] investigated the Effect of Solid Volume Concentration on Rheological Properties of non -Newtonian fluid.

From the above works review, it is evidently explaining that the investigation of nano, hybrid and ternary nanofluid are carried out for the thermal behavior and flow of fluid in stretching sheet with various boundary conditions. Thus, an honest attempt has been done to study the analyzing of heat and mass transfer in unsteady cases of ternary nanofluid flow over a stretched surface while considering the combined influence of a magnetic field, thermal stratification, and solutal stratification. This problem is solved numerically by using Runge-Kutta Fehlberg method. The main novelty of this problem is the combination of homogeneous and heterogeneous reactions fluid flow over stretching sheet. Additionally, statistical tool that is RSM is utilized to analyze the rate of heat transfer of the fluid flow. This lack of research in the current literature highlights a chance for upcoming studies to explore the complex relationships among these variables and how they affect the dynamics and transportation phenomena of ternary nanofluids.

The present work will be help to answer the following novel questions like:

- What is the impact of double stratification on temperature and concentration?
- What is the effect of ternary hybrid nanofluid over a stretching sheet?
- What is the impact of magnetic field on velocity and temperature in the presence of double stratification?
- Which elements are significant for enhancing the rate of heat transfer?

2. Problem formulation

A two-dimensional unsteady, incompressible and thin film of a ternary nanofluid past a stretching sheet which is along the x-axis is considered as depicted in Fig. 1. An even magnetic field B_0 is applied perpendicular to the x-axis. Tin film flow occurs as a result of sheet stretching. The liquid film thickness is given by h(t), whereas the surface temperature and velocity of the stretched sheet are denoted by Uw and Ts, respectively. Following Cao al. [39] and Ying-Qing et al. [54], modification of the Buongiorno's Nanofluid Model was considered in the energy equation and concentration equation since thermo-migration and haphazard motion of nanoparticles occur due to variation in the concentration. Under the above constraints, the governing equations are considered as follows [37,38,41]:

Governing equations:

$$\frac{\partial u_1^*}{\partial x}+\frac{\partial u_2^*}{\partial y}=0, \tag{1}$$

$$\frac{\partial u_1^*}{\partial t}+u_1^*\frac{\partial u_1^*}{\partial x}+u_2^*\frac{\partial u_1^*}{\partial y}=\frac{\mu_{nf}^*}{\rho_{nf}^*}\frac{\partial^2 u_1^*}{\partial y^2}-\frac{\sigma_{nf}^*}{\rho_{nf}^*}B(t)^2u_1^*, \tag{2}$$

$$\frac{\partial T^*}{\partial t}+u_1^*\frac{\partial T^*}{\partial x}+u_2^*\frac{\partial T^*}{\partial y}=\alpha_{nf}^*\frac{\partial^2 T^*}{\partial y^2}+\frac{\mu_{nf}^*}{\rho_{nf}^*C_p^*}\left(\frac{\partial u_1^*}{\partial y}\right)^2+\tau\left[D_B\frac{\partial C}{\partial y}\frac{\partial T^*}{\partial y}+\left(\frac{D_T}{T_\infty^*}\right)\left(\frac{\partial T^*}{\partial y}\right)^2\right], \tag{3}$$

$$\frac{\partial C^*}{\partial t}+u_1^*\frac{\partial C^*}{\partial x}+u_2^*\frac{\partial C^*}{\partial y}=D_B\left(\frac{\partial^2 C^*}{\partial y^2}\right)+\left(\frac{D_T}{T_\infty^*}\right)\frac{\partial^2 T^*}{\partial y^2} \tag{4}$$

For this study, the boundary conditions are [41]:

$$\begin{aligned} &y=0\rightarrow u_1^*=U_w, u_2^*=0, T^*=T_w, C^*=C_w,\\ &y=h(t)\rightarrow\frac{\partial u_1^*}{\partial y}=0,\frac{\partial T^*}{\partial y}=0, u_2^*=\frac{\partial h}{\partial t},\frac{\partial C^*}{\partial y}=0 \end{aligned} \tag{5}$$

The physical significance of slip and convective boundary conditions are, in slip boundary condition fluid does not stick completely to a solid surface, allowing for some relative motion at the boundary. In convective boundary condition represents heat transfer at a surface where both conduction through the solid and convection into the surrounding fluid (ternary nanofluid) are present.

Similarity transformations are:

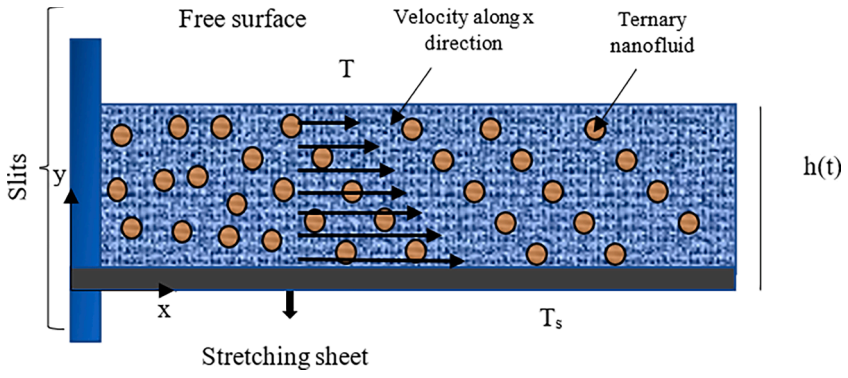

Fig. 1. Physical model.

$$\eta = \frac{1}{\beta}\sqrt{\frac{b}{\nu_f(1-\alpha t)}}y, \psi = \beta\sqrt{\frac{\nu_f b}{(1-\alpha t)}}xf(\eta), \theta(\eta) = \frac{T^* - T_\infty}{T_w - T_0}, \varphi(\eta) = \frac{C^* - C_\infty}{C_w - C_0} \tag{6}$$

Where, ψis a stream function which determines the fluid flow pattern and is defined as ${u_1}^* = \frac{\partial\psi}{\partial y}$and ${u_2}^* = -\frac{\partial\psi}{\partial x}$, so that the continuity equation satisfies identically. By substituting the above similarity variables Eq. (6) into Eqs. (2)–(5), the below nonlinear ordinary differential equations are obtained.

$$\beta^2\left[S\left(f'(\eta)+\frac{1}{2}\eta f''(\eta)\right)+[f'(\eta)]^2 - f''(\eta)f(\eta)+Z_2Mf'(\eta)\right] = Z_1 f'''(\eta) \tag{7}$$

$$\beta^2\begin{bmatrix} S\left(\theta(\eta)+\theta'(\eta)\frac{\eta}{2}+S_t\right)+f'(\eta)S_t \\ +f'(\eta)\theta(\eta) - f(\eta)\theta'(\eta)\end{bmatrix} = \begin{bmatrix}\frac{1}{\mathrm{Pr}}Z_3(\theta''(\eta))+\frac{1}{\mathrm{Pr}}Z_3Ec[f'''(\eta)]^2 \\ +\varphi'(\eta)\theta'(\eta)Nb + Nt[\theta'(\eta)]^2\end{bmatrix} \tag{8}$$

$$\beta^2\left[S\left(\varphi(\eta)+\varphi'(\eta)\frac{1}{2}\eta+S_m\right)+f'(\eta)\varphi(\eta)+S_m f'(\eta) - f(\eta)\varphi'(\eta)\right] = \frac{1}{Sc}\left[\varphi''(\eta)+\theta''(\eta)\frac{Nt}{Nb}\right] \tag{9}$$

Substituting Eq. (6) in Eq. (5) the non-dimensional boundary conditions are obtained:

$$\begin{aligned} &f(\eta) = 0, f'(\eta) = 1, \theta(\eta) = 1 - S_t, \varphi(\eta) = 1 - S_m \ \mathbf{at}\eta = 0 \\ &f(\eta) = \frac{S}{2}, \theta'(\eta) = 0, \varphi'(\eta) = 0\mathbf{at}\eta = 1\end{aligned} \tag{10}$$

Dimensionless constants are:

$$\begin{aligned} &B(t) = \frac{B_0}{\sqrt{(1-\alpha t)}}, S_m = \frac{E}{D}, S = \frac{\alpha}{b}, Sc = \frac{\nu_f}{D_B}, Ec = \frac{U}{(T_w - T_0){C_p}^*}, Nb = \frac{\tau D_B(C_w - C_0)}{\nu_f}, \\ &Nt = \frac{\tau D_T(T_w - T_0)}{T_\infty \nu_f}, S_t = \frac{B}{A}, \mathrm{Pr} = \frac{\alpha_f}{\nu_f}, M = \frac{\sigma_f {B_0}^2}{\rho_f b}\end{aligned} \tag{11}$$

2.1. Derived quantities

The skin friction coefficient, Nusselt number, and Sherwood number are the physical quantities related to this issue:

$$C_f = \frac{\tau_w}{\rho_f {U_w}^2}, Nu = \frac{x^* q_w}{k_f^*(T_w - T_0)} and Sh = \frac{x^* J_w}{D_B(C_w - C_0)} \tag{12}$$

Where,

$$\tau_w = \mu_{tnf}\left(\frac{\partial {u_1}^*}{\partial y^*}\right)_{y^*=0}, q_w = -k_{tnf}\left(\frac{\partial T^*}{\partial y^*}\right)_{y^*=0} and J_w = -D_B\left(\frac{\partial C^*}{\partial y^*}\right)_{y^*=0} \tag{13}$$

Substituting Eq. (13) in Eq. (12), the dimensionless physical quantities are as follows:

$$C_{fx}{\mathrm{Re}_x}^{-1/2} = \frac{1}{\beta(1-\phi_1)^{2.5}(1-\phi_2)^{2.5}(1-\phi_3)^{2.5}}f''(0), Nu_x{\mathrm{Re}_x}^{-1/2} = -\frac{k_{tnf}}{\beta k_f}\frac{1}{(1-S_t)}\theta'(0) and$$
$$Sh_x{\mathrm{Re}_x}^{-1/2} = -\frac{1}{\beta}\left(\frac{1}{1-S_m}\right)\varphi'(0).$$

2.2. Numerical procedure

Computing numerical solutions using the fourth-order Runge-Kutta-Fehlberg method in Mathematica allows us to tackle the nonlinear differential equations and related boundary conditions that were previously discussed. By including a midpoint in the step, this methodology improves accuracy by one order of magnitude when compared to the Euler method. As a result, a numerical strategy that works well for solving the problems is the midway method. The detail of the Runge–Kutta–Fehlberg fourth fifth order numerical method is given below:

$$k_0 = f(x_i, y_i),$$

$$k_1 = f\left(x_i + \frac{1}{4}h, y_i + \frac{1}{4}hk_0\right),$$

$$k_2 = f\left(x_i + \frac{3}{8}h, y_i + \left(\frac{3}{32}k_0 + \frac{9}{32}k_1\right)h\right),$$

$$k_3 = f\left(x_i + \frac{12}{13}h, y_i + \left(\frac{1932}{2197}k_0 - \frac{7200}{2197}k_1 + \frac{7296}{2197}k_2\right)h\right),$$

$$k_4 = f\left(x_i + h, y_i + \left(\frac{439}{216}k_0 - 8k_1 + \frac{3860}{513}k_2 - \frac{845}{4104}k_3\right)h\right),$$

$$k_5 = f\left(x_i + \frac{1}{2}h, y_i + \left(-\frac{8}{27}k_0 + 2k_1 - \frac{3544}{2565}k_2 + \frac{1859}{4104}k_3 - \frac{11}{40}k_4\right)h\right),$$

$$y_{i+1} = y_i + \left(\frac{25}{216}k_0 + \frac{1408}{2565}k_2 + \frac{2197}{4104}k_3 - \frac{1}{5}k_4\right)h,$$

$$z_{i+1} = z_i + \left(\frac{16}{135}k_0 + \frac{6656}{12825}k_2 + \frac{28561}{56430}k_3 - \frac{9}{50}k_4 + \frac{2}{55}k_5\right)h,$$

Where y is the fourth-order Runge-Kutta and $z$is the fifth order Runge-Kutta. An estimate of the error can be obtained by subtracting the two values obtained. If the error exceeds a specific threshold, the results can be recalculated using smaller step size. The approach to estimating the new step size is given below. The step size and the convergence criterion are taken 10^{-6} and $\Delta\eta = 0.001$respectively.

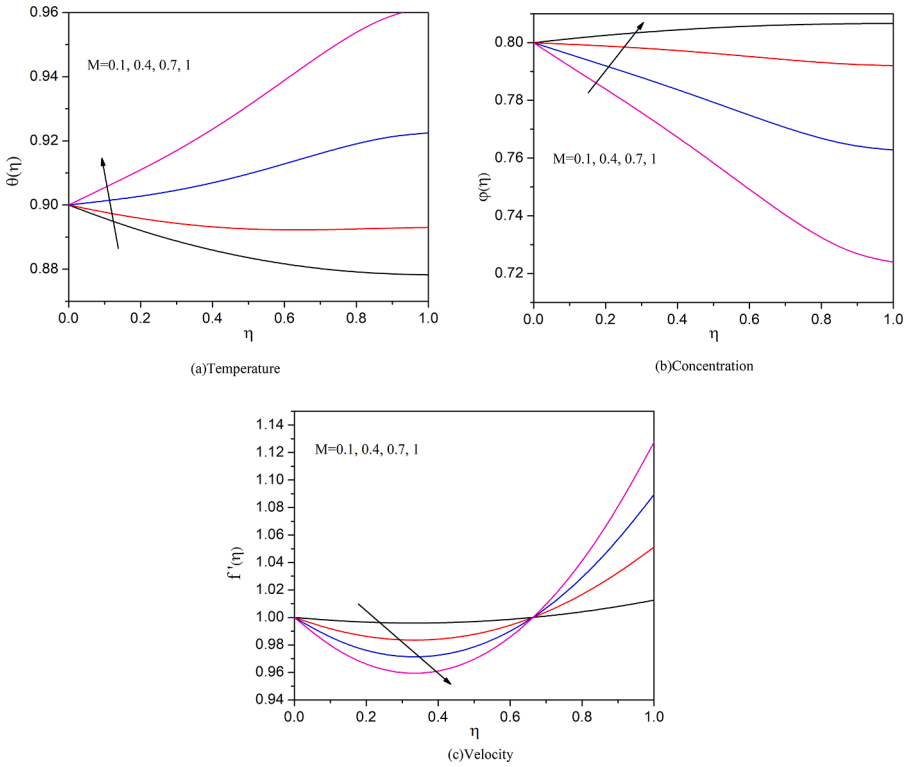

Fig. 2. Effect of Magnetic field.

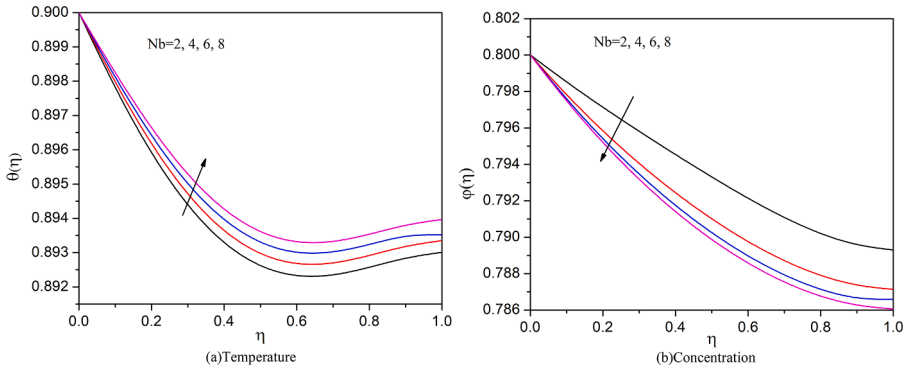

Fig. 3. Effect of Brownian motion parameter.

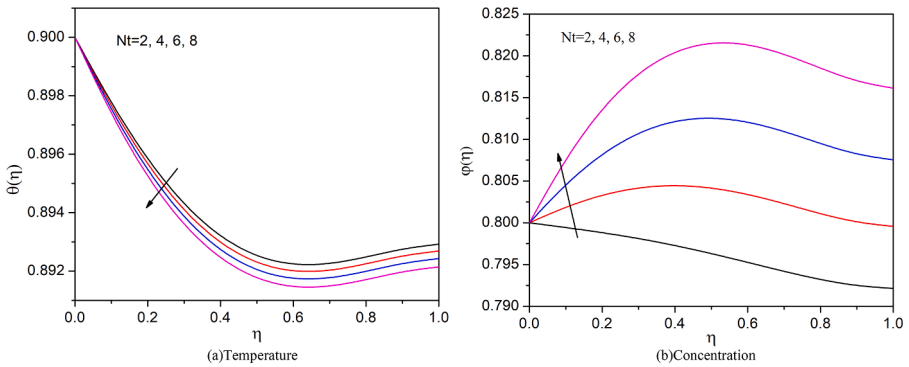

Fig. 4. Effect of thermophoresis parameter.

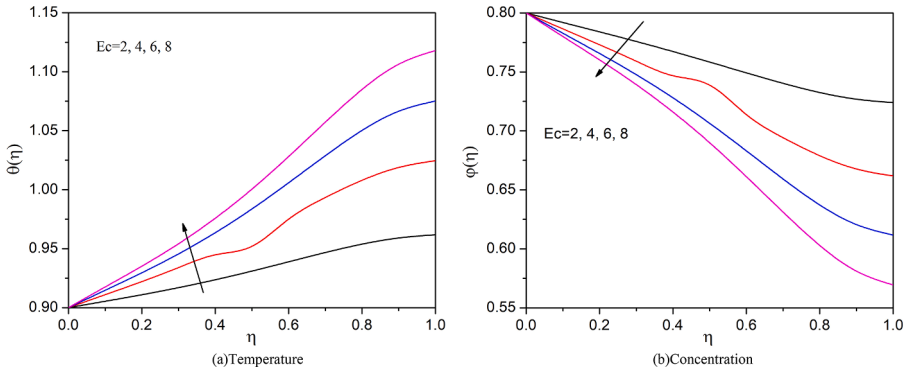

Fig. 5. Effect of Eckert number.

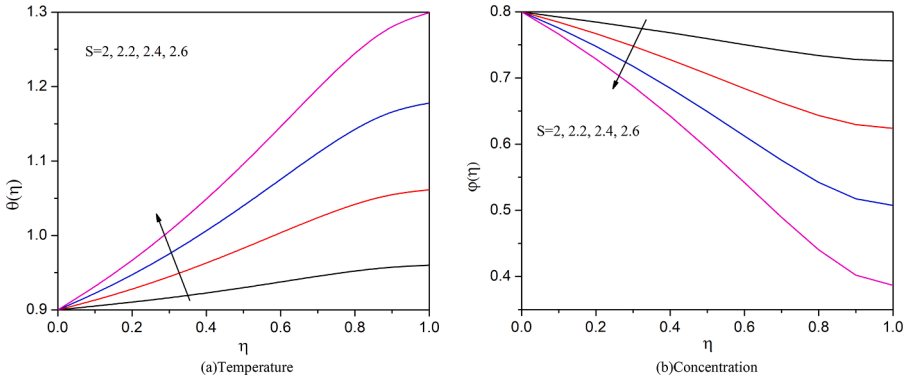

Fig. 6. Effect of Unsteadiness parameter.

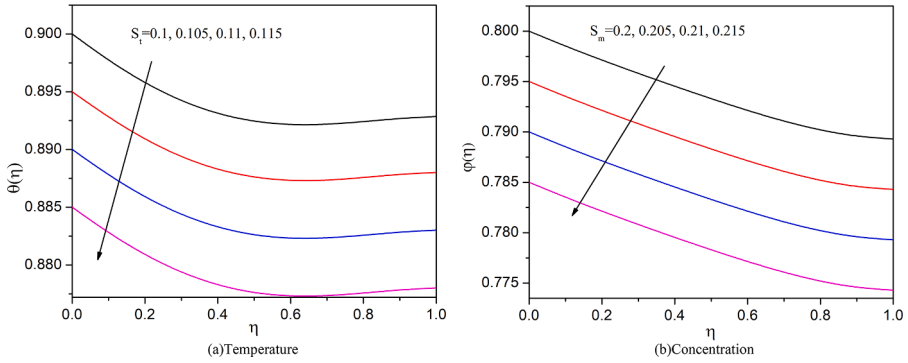

Fig. 7. Effect of thermal stratification (St) and mass stratification (Sm).

3. Results and discussion

3.1. Analysis of results

Various schemes exist [45–50] to report flow field solutions but the mathematical theories of the RKF-45 and RSM provide highly accurate solutions for the heat and mass transfer problems, which are presented in Section 2. The solution is obtained by using RKF-45 technique. The open software Mathematica is used for our computational work and the graphs are plotted by using Origin software. The results obtained are compared with Fakour et al. [41] they are in good agreement. From Figs. 2–8, the effects of fluid flow parameters are studied by using RKF-45 and in the Fig. 9, the effects of three various parameters of fluid flow and the effect of Nusselt number are studied by using RSM model. Tables 1–3 denotes the thermophysical properties of nano, hybrid and ternary nanofluids and in Table 4 the thermophysical values of ternary nanoparticles and base fluid can be seen. Table 5 offers the comparative study. Table 6 denotes the effect of three different parameters and Table 7 denotes the Nusselt number values for the combination of three different parameters values and also, the Table 8 gives the co-efficient values of the parameters, that is ANOVA table.

3.2. Discussion of results

In this segment, an in-depth analysis has been conducted, encompassing numerical computations for significant parameters related to velocity, temperature, and concentration profiles in steady scenarios of nanofluid. Figs. 2-9 graphically display the results. The influence of relevant parameters on hydrodynamic, thermal, and solutal boundary layers has been acknowledged, and the results compared to those of Mehdi Fakour et al. [41] are shown in Table 5. The effect of the magnetic field strength (M) on the distributions of velocity, temperature, and

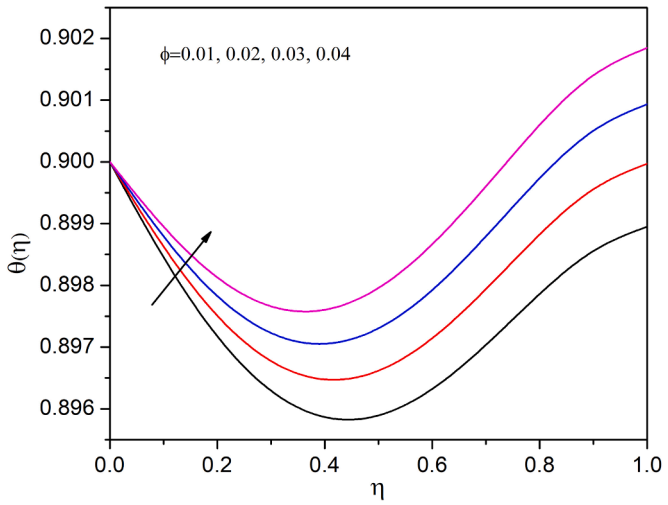

Fig. 8. Effect of solid volume fraction on temperature.

concentration is illustrated graphically in Fig. 2. Theoretically, the fluid's velocity distribution should shrink significantly as (M) values rise. The Lorentz force arises in the electrically conducting fluid region when a magnetic field is present, leading to resistance against the flow direction and a decrease in velocity in the sketches. The thickness of the thermal and solutal boundary layers increases as the values rise, particularly in the steady state compared to the unsteady state. This occurs because the fluid must exert additional effort, which can be transformed into thermal energy, raising the fluid's temperature.

In Fig. 3, it is noticed that how the Brownian motion parameter affects the concentration and temperature profiles of ternary nanoparticles A discernible trend is experimental., wherein the concentration of ternary nanoparticles in the fluid reduces as the Brownian motion of these nanoparticles increases. It is noteworthy to highlight the intriguing observation that Brownian motion, occurring at molecular and nanoscale levels, plays an essential role in influencing the thermal behavior of the nanoparticles in conjunction with the fluid particles. This tends to a reduction in the solutal thermal boundary layer thickness, a phenomenon directly attributable to the effects of Brownian motion. Brownian

Table 1
Properties of nanofluid [42].

Properties	Nanofluid
Density	$\rho_{nf} = (1-\phi_{AI})\rho_f + \phi_{AI}\rho_{AI}$
Heat capacity	$(\rho C_p)_{nf} = (1-\phi_{AI})(\rho C_p)_f + \phi_{AI}(\rho C_p)_{AI}$
Viscosity	$\mu_{nf} = \frac{\mu_f}{(1-\phi_{AI})^{2.5}}$
Thermal conductivity	$\frac{k_{nf}}{k_f} = \frac{k_{AI}+2k_f-2\phi_{AI}(k_f-k_{AI})}{k_{AI}+2k_f+\phi_{AI}(k_f-k_{AI})}$

Table 2
Properties of Hybrid nanofluid [43].

Properties	Hybrid nanofluid
Density	$\rho_{hnf} = (1-\phi_{Si})[(1-\phi_{AI})\rho_f + \phi_{AI}\rho_{AI}] + \phi_{Si}\rho_{Si}$
Heat capacity	$(\rho C_p)_{hnf} = (1-\phi_{Si})[(1-\phi_{AI})(\rho C_p)_f + \phi_{AI}(\rho C_p)_{AI}] + \phi_{Si}(\rho C_p)_{Si}$
Viscosity	$\mu_{hnf} = \frac{\mu_{nf}}{(1-\phi_{AI})^{2.5}(1-\phi_{Si})^{2.5}}, \mu_{nf} = \frac{\mu_f}{(1-\phi_{AI})^{2.5}}$
Thermal conductivity	$\frac{k_{hnf}}{k_{nf}} = \frac{k_{Si}+2k_{nf}-2\phi_{Si}(k_{nf}-k_{Si})}{k_{Si}+2k_{nf}+\phi_{Si}(k_{nf}-k_{Si})}, \frac{k_{nf}}{k_f} = \frac{k_{AI}+2k_f-2\phi_{AI}(k_f-k_{AI})}{k_{AI}+2k_f+\phi_{AI}(k_f-k_{AI})}$

Table 3
Properties of Ternary nanofluid [44].

Properties	Ternary nanofluid
Density	$\rho_{tnf} = \phi_{AI}\rho_{AI} + (1-\phi_{AI})[(1-\phi_{Si})\{(1-\phi_{Zn}) + \phi_{Zn}\rho_{Zn}\} + \phi_{Si}\rho_{Si}]$
Heat capacity	$(\rho C_p)_{tnf} = \phi_{AI}(\rho C_p)_{AI} + (1-\phi_{AI})\left[\begin{array}{l}(1-\phi_{Si})\{(1-\phi_{Zn}) + \phi_{Zn}(\rho C_p)_{Zn}\} \\ +\phi_{Si}(\rho C_p)_{Si}\end{array}\right]$
Viscosity	$\mu_{tnf} = \frac{\mu_{hnf}}{(1-\phi_{AI})^{2.5}(1-\phi_{Si})^{2.5}(1-\phi_{Zn})^{2.5}}, \mu_{hnf} = \frac{\mu_{nf}}{(1-\phi_{AI})^{2.5}(1-\phi_{Si})^{2.5}}, \mu_{nf} = \frac{\mu_f}{(1-\phi_{AI})^{2.5}}$
Thermal conductivity	$\frac{k_{tnf}}{k_{hnf}} = \frac{k_{Zn}+2k_{hnf}-2\phi_{Zn}(k_{hnf}-k_{Zn})}{k_{Zn}+2k_{hnf}+\phi_{Zn}(k_{hnf}-k_{Zn})}, \frac{k_{hnf}}{k_{nf}} = \frac{k_{Si}+2k_{nf}-2\phi_{Si}(k_{nf}-k_{Si})}{k_{Si}+2k_{nf}+\phi_{Si}(k_{nf}-k_{Si})}, \frac{k_{nf}}{k_f} = \frac{k_{AI}+2k_f-2\phi_{AI}(k_f-k_{AI})}{k_{AI}+2k_f+\phi_{AI}(k_f-k_{AI})}$

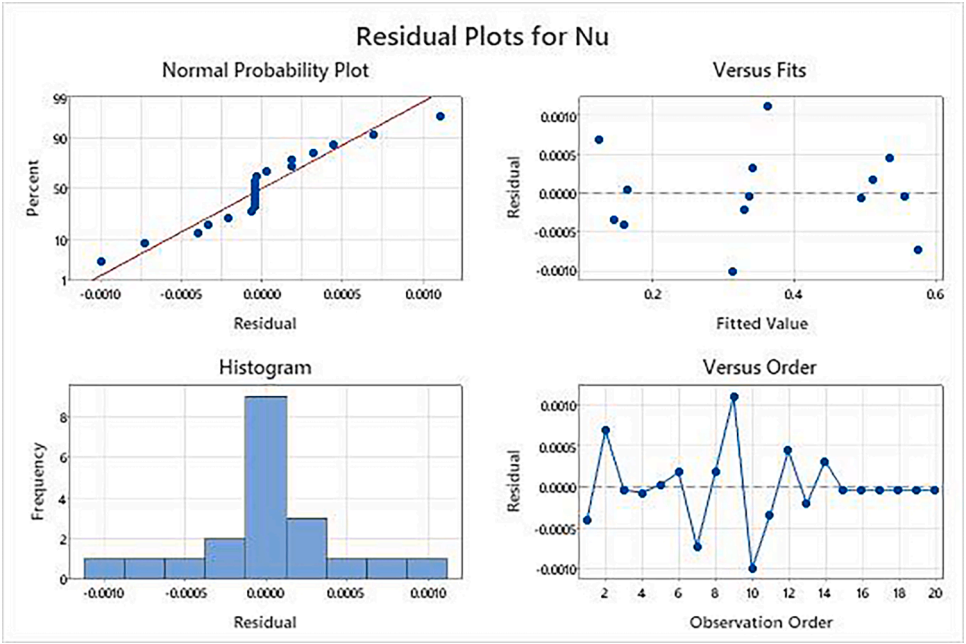

Fig. 9. Residual plot of Nu.

Table 4
Thermophysical properties of nanoparticles [52–53].

Property	Water	Aluminium (AI)	Silicon (Si)	Zinc (Zn)
ρ	997.1	2700	2328	7140
k	0.613	237	148	116
C_p	4179	910	710	389
σ	0.05	39.6×10^6	0.2×10^6	1.69×107

Table 5
Comparison study.

S	$f(1)$	
	Present study	Fakour et al. [41]
0.25	0.140191	0.140187
0.5	0.257010	0.257009
0.75	0.392534	0.392523
1	0.514020	0.514019
1.25	0.640197	0.640187
1.5	0.757011	0.757009
1.75	0.89253	0.89252
2	1.00000	1.00000

Table 6
The impact of different parameter values.

Parameter	Symbol	Level		
		−1	0	+1
$2 \leq Nb \leq 6$	J_1	2	4	6
$2.2 \leq S \leq 2.6$	J_2	2.2	2.4	2.6
$0.005 \leq \phi \leq 0.015$	J_3	0.005	0.01	0.015

Table 7
An investigational strategy based on CCD.

Iteration	Coded values			Real values			Response
	J_1	J_2	J_3	Nb	S	ϕ	Nu
1	−1	−1	−1	2	2.2	0.005	0.158906
2	1	−1	−1	6	2.2	0.005	0.124917
3	−1	1	−1	2	2.6	0.005	0.555999
4	1	1	−1	6	2.6	0.005	0.495525
5	−1	−1	1	2	2.2	0.015	0.165069
6	1	−1	1	6	2.6	0.015	0.512466
7	−1	1	1	2	2.6	0.015	0.572974
8	1	1	1	6	2.6	0.015	0.512466
9	−1	0	0	2	2.4	0.010	0.362730
10	1	0	0	6	2.4	0.010	0.312372
11	0	−1	0	4	2.2	0.010	0.144928
12	0	1	0	4	2.6	0.010	0.535732
13	0	0	−1	4	2.4	0.005	0.329080
14	0	0	1	4	2.4	0.015	0.340819
15	0	0	0	4	2.4	0.010	0.336595
16	0	0	0	4	2.4	0.010	0.336595
17	0	0	0	4	2.4	0.010	0.336595
18	0	0	0	4	2.4	0.010	0.336595
19	0	0	0	4	2.4	0.010	0.336595
20	0	0	0	4	2.4	0.010	0.336595

motion refers to the unpredictable movement of nanoparticles suspended in the base fluid, primarily influenced by the rapid motion of atoms or molecules within the fluid. It is important to note that the extent of Brownian motion is associated with the size of the nanoparticles, which typically exist in the form of agglomerates and aggregates.

Fig. 4 substantiates the influence of the thermophoresis parameter on both temperature and concentration profiles. The depicted data highlights a clear and consistent impact of the thermophoresis parameter on the distribution of ternary nanoparticles and temperature within the system. Notably, the rapport between the thermophoresis parameter and the concentration distribution of ternary nanoparticles exhibits a monotonic trend, indicating a heightened sensitivity of particle concentration to increase in the thermophoresis parameter. An important point to note from the figure is the consistent decrease in the extent of the concentration gradient at the surface as the thermophoresis parameter reaches higher values. This indicates that particles' concentration becomes more sensitive to changes in the thermophoresis parameter, leading to a more noticeable impact on the concentration distribution. Moreover, the decrease in the temperature distribution can be explained as a result of the higher thermophoresis parameter value. The reason behind this is that, as thermophoresis impedes the mass transfer of nanofluids, it also reduces the temperature distribution. In Fig. 5(a), the graphical representation sheds light on the noteworthy impact of the Eckert number on ternary nanofluid temperature. The observed trends reveal a distinct enhancement in parameters as the Eckert number experiences an increase.

This phenomenon is attributed to the heightened kinetic energy, which, in turn, elevates the conversion of energy to enthalpy within the nanofluid system. As the values of the Eckert number rise, there is a consequential augmentation in the fluid temperature. This can be accredited to the increased kinetic energy influencing the energy-to-enthalpy conversion process. The heightened kinetic energy essentially contributes to a more substantial rise in the overall temperature. Simultaneously, the thermal boundary layer thickness experiences an upsurge as the Eckert parameter values rise. This observation aligns with the enhanced temperature, indicating a broader span over which thermal effects manifest within the boundary layer. The decrease in concentration with an increase in the Eckert number can be attributed to the interplay between the thermal and kinetic aspects of the fluid dynamics which is noticed in Fig. 5(b). As the Eckert number increases, it signifies a higher proportion of kinetic energy relative to enthalpy in the fluid flow. Both (a) and (b) of Fig. 6 show how the ternary nanofluid temperature and concentration profile is affected by the unsteadiness parameter. As the unsteadiness upsurges, the thermal characterizes of the ternary nanofluid exhibit variations over time. This implies that the thermal characteristics of the system are influenced by temporal changes, and the temperature distribution evolves dynamically.

The unsteadiness parameter essentially signifies the degree to which the system deviates from a steady-state condition, and its increase introduces a time-dependent element to the thermal behavior of the nanofluid. Similarly, the concentration profiles in Fig. 6(b) of the ternary nanofluid are affected by changes in the unsteadiness parameter. An increase in the unsteadiness parameter suggests a more dynamic and time-evolving concentration distribution. The temporal variations may be attributed to factors such as fluctuations in flow conditions or external influences that introduce unsteadiness to the system. Fig. 7(a) provides a summary of the temperature characteristics for a range of thermal stratification parameters, illustrating the variations in temperature across the considered range of parameter values. In highly stratified systems, conductive heat transfer within each layer can become more dominant than convective heat transfer between layers. Conductive heat transfer is typically less efficient than convective heat transfer. Therefore, an increase in thermal stratification may lead to a decrease in the overall efficiency of heat transfer, resulting in a lower temperature. The effect of Mass stratification on concentration can be studied from Fig. 7(b). The higher mass stratification hinders the mixing of fluid between different layers. This reduced mixing restricts the transfer of particles or solutes between layers, preventing the equalization of concentrations. As a result, regions with higher concentrations may not effectively mix with regions of lower concentrations, leading to an overall decrease in concentration.

The increase in temperature with an increase in the solid volume fraction of ternary nanofluids can be observed in Fig. 8. The addition of particles improves the heat conduction properties of the ternary nanofluid. Ternary Nanoparticles facilitate a more efficient transfer of heat from particles to their environment. This improved heat conduction

Table 8
Analysis of Variance (ANOVA) of Nu_x.

Source	Degrees of freedom	Adjusted sum of squares	Adjusted mean squares	F-value	p-value	Coefficients
Model	9	0.366194	0.040688	103,216.78	0.000	0.336633
Linear	3	0.318001	0.106000	268,898.18	0.000	–
Nb	1	0.004251	0.004251	10,784.99	0.000	−0.024124
S	1	0.259213	0.259213	657,564.91	0.000	0.195008
Phi	1	0.000230	0.000230	582.39	0.000	0.005606
Square	3	0.000051	0.000017	43.33	0.000	–
Nb^2	1	0.000002	0.000002	5.05	0.048	0.000860
S^2	1	0.000036	0.000036	90.49	0.000	0.003639
ϕ^2	1	0.000008	0.000008	20.72	0.001	−0.001741
2-Way Interaction	3	0.000381	0.000127	321.81	0.000	–
Nb*S	1	0.000203	0.000203	514.94	0.000	−0.006339
Nb*ϕ	1	0.000000	0.000000	0.83	0.384	−0.000244
S*ϕ	1	0.000045	0.000045	114.16	0.000	0.002985
Error	10	0.000004	0.000000	-	-	–
Lack-of-Fit	4	0.000004	0.000001	–	–	–
Pure Error	6	0.000000	0.000000	-	-	–
Total	19	0.366198		-	-	–

results in a faster and more effective dissipation of heat within the nanofluid, contributing to an increase in temperature.

4. Response surface methodology (RSM)

The RSM is an operative tool for developing empirical correlations between numerous constraints. It is very beneficial for assessing processes with numerous variables, since it enables one to examine the input elements that have the least and most influence on the outputs. RSM seeks to optimize responses; in this study, the effect of chosen input parameters, namely Nb, S, and, ϕ on Nu is determined. Table 6 shows how the input parameters are adjusted within a specific range and at three levels.

The next step, as indicated in Table 7, is to create a statistical model with 20 runs for the selected input parameters. A second-order multinomial is used to represent the interaction effects of the input parameters on the response.

$$Nu_x = Z_0 + Z_1 Nb + Z_2 Sc + Z_3 \phi + Z_{11} Nb^2 + Z_{22} S^2 + Z_{33} \phi^2 + Z_{12} NbS + Z_{13} Nb\phi + Z_{14} \phi S.$$

In the provided context, the model is described using a second-order polynomial equation where Z_0 represents the intercept, Z_i denotes the linear coefficients, Z_{ii} represents the quadratic coefficients, and Z_{ij} denotes the interaction coefficients. The polynomial equation's terms are influenced by the regression coefficients, which aid in illustrating the connections and interplay between the input parameters. CCD is used to fit this polynomial. This design has six axial points, eight cube points, and six centre points, enabling a total of twenty experimental runs. The layout of the design makes it easier to estimate the polynomial model's regression coefficients and to effectively explore the factor space. In regression analysis, an Analysis of Variance (ANOVA) table is a useful tool to assess the overall significance of a regression model. It decomposes the total variation in the response variable into components attributable to the predictors (regression) and the residual error [51]. Analysis of Variance (ANOVA) is used to verify the developed model's practical applicability and consequence. The findings are shown in Table 8. A larger S^2 number indicates that all of the variations in Nu can be explained by the established model. The F-statistic and corresponding p-value help in determining whether the overall regression model is statistically significant. Z-values for model terms are analyzed using a significance threshold (α) of 0.05. The accuracy of the model is noted from the value $R^2 = 100$ %. After eliminating the non-significant factors from Table 8, the model for Nu is as follows:

$$Nu_x = 0.336633 - 0.024124Nb + 0.195008S + 0.005606\phi + 0.000860Nb^2 + 0.003639S^2 - 0.001741\phi^2 - 0.006339Nb \times S - 0.000244Nb \times \phi + 0.002985S \times \phi.$$

Fig. 9 shows the residual plots that were produced after the Analysis for *Nu* was completed. Given that the probability plot for regression displays a favourable condition, the residuals have a normal distribution. An even distribution is also shown by the residual histogram. Interestingly, the largest residuals are found. Despite this, it can be said that the developed model is useful and exhibits a good fit based on the general pattern and residuals' properties. The behavior of the residuals indicates that the model can capture the variability in the response variable *Nu*, which supports the validity and suitability of the developed quadratic model for particular research.

5. Conclusions

The thermally magnetized hybrid ternary nanofluid flow is mathematically modelled over a stretched surface along with heat and mass transfer aspects. Unsteady fluid flow is carried with the effects of temperature and mass stratification. In order to resolve the consequent ordinary differential equations that are not linear, the fourth-fifth order Runge-Kutta-Fehlberg method is utilized. The findings are presented through both graphical representations and numerical solutions, and yield the following significant outcomes:

- By increasing magnetic parameter, the temperature and concentration of the fluid increases, the momentum of velocity decreases.
- The heat transfer enhances by increasing the Brownian motion parameter and Eckert number, the concentration decreases for both the parameters.
- By upsurging the thermophoresis parameter, the heat transfer of the fluid decreases and mass transfer of the fluid increases.
- The behavior of the residuals indicates that the model by using RSM can capture the variability in the response variable namely Nusselt number.

- From RSM it is noticed that adjusted R-squared and R-squared are obtained as 100 % accuracy of the mathematical model.

CRediT authorship contribution statement

Tanuja T. N: Validation, Resources, Methodology, Investigation, Formal analysis. **Kavitha L:** Writing – original draft, Methodology, Investigation, Formal analysis, Data curation. **Khalil Ur Rehman:** Writing – original draft, Visualization, Methodology, Investigation. **S.V. K Varma:** Validation, Supervision, Software, Methodology. **Wasfi Shatanawi:** Writing – review & editing, Visualization, Supervision, Methodology. **G.V. Kumar:** Writing – review & editing, Visualization, Validation, Resources. **Zeeshan Asghar:** Writing – review & editing, Visualization, Validation, Methodology.

Declaration of competing interest

Authors have no conflict of Interest at this stage.

Acknowledgement

The authors would like to thank Prince Sultan University, Saudi Arabia, for the technical support through the TAS research lab.

Data availability

No data was used for the research described in the article.

References

[1] L.J. Crane, Flow past a stretching plate, ZeitschriftfürangewandteMathematik und Physik ZAMP 21 (4) (1970) 645–647, https://doi.org/10.1007/BF01587695.
[2] P.S. Gupta, A.S. Gupta, Heat and mass transfer on a stretching sheet with suction or blowing, Can. J. Chem. Eng. 55 (6) (1977) 744–746, https://doi.org/10.1002/cjce.5450550619.
[3] C.-K. Chen, M.-I. Char, Heat transfer of a continuous, stretching surface with suction or blowing, J. Math. Anal. Appl. 135 (2) (1988) 568–580, https://doi.org/10.1016/0022-247X(88)90172-2.
[4] B.K. Dutta, P. Roy, A.S. Gupta, Temperature field in flow over a stretching sheet with uniform heat flux, Int. Commun. Heat Mass Transf. 12 (1) (1985) 89–94, https://doi.org/10.1016/0735-1933(85)90010-7.
[5] K. Bhattacharyya, S. Mukhopadhyay, G.C. Layek, Unsteady MHD boundary layer flow with diffusion and first-order chemical reaction over a permeable stretching sheet with suction or blowing, Chem. EngCommun. 200 (3) (2013) 379–397, https://doi.org/10.1080/00986445.2012.712577.
[6] F.K. Tsou, E.M. Sparrow, R.J. Goldstein, Flow and heat transfer in the boundary layer on a continuous moving surface, Int. J. Heat Mass Transf. 10 (2) (1967) 219–235, https://doi.org/10.1016/0017-9310(67)90100-7.
[7] D. Bhukta, G.C. Dash, S.R. Mishra, Heat and mass transfer on MHD flow of a viscoelastic fluid through porous media over a shrinking sheet, Int. Sch. Res. Notice. 2014 (2014) 1–11, https://doi.org/10.1155/2014/572162.
[8] K. Das, Nanofluid flow over a non-linear permeable stretching sheet with partial slip, J. Egypt. Math. Soc. 23 (2) (2015) 451–456, https://doi.org/10.1016/j.joems.2014.06.014.
[9] R. Cortell, Viscous flow and heat transfer over a nonlinearly stretching sheet, Appl. Math. Comput. 184 (2) (2007) 864–873, https://doi.org/10.1016/j.amc.2006.06.077.
[10] S. Nadeem, R.U. Haq, N.S. Akbar, MHD three-dimensional boundary layer flow of casson nanofluid past a linearly stretching sheet with convective boundary condition, IEEE. Trans. Nanotechnol. 13 (1) (2014) 109–115, https://doi.org/10.1109/TNANO.2013.2293735.
[11] M. Mustafa, J.A. Khan, Model for flow of Casson nanofluid past a non-linearly stretching sheet considering magnetic field effects, AIP. Adv. 5 (7) (2015), https://doi.org/10.1063/1.4927449.
[12] W.N. Mutuku, O.D. Makinde, Double stratification effects on heat and mass transfer in unsteady MHD nanofluid flow over a flat surface, Asia Pac. J. Comput. Eng. 4 (1) (2017) 2, https://doi.org/10.1186/s40540-017-0021-2.
[13] K. Mehmood, S. Hussain, M. Sagheer, Mixed convection flow with non-uniform heat source/sink in a doubly stratified magnetonanofluid, AIP. Adv. 6 (6) (2016), https://doi.org/10.1063/1.4955157.
[14] S.U. S, E.J.A. Choi, Enhancing Thermal Conductivity of Fluids with Nanoparticles, 1995. United States: N p.
[15] M. Sheikholeslami, D.D. Ganji, Heat transfer of Cu-water nanofluid flow between parallel plates, Powder Technol. 235 (2013) 873–879, https://doi.org/10.1016/j.powtec.2012.11.030.
[16] T. Hayat, M. Waqas, S.A. Shehzad, A. Alsaedi, On model of Burgers fluid subject to magneto nanoparticles and convective conditions, J. Mol. Liq. 222 (2016) 181–187, https://doi.org/10.1016/j.molliq.2016.06.087.
[17] O.D. Makinde, A.S. Eegunjobi, MHD flow of a reacting and radiating nanoliquid past an inclined heated permeable plate: analysis of entropy generation, *Latin Am. Appl. Res. - Int. J.* 51 (4) (2021) 269–276, https://doi.org/10.52292/j.laar.2021.715.
[18] S.M. Seyyedi, A.S. Dogonchi, M. Hashemi-Tilehnoee, M. Waqas, D.D. Ganji, Entropy generation and economic analyses in a nanofluid filled ʟ-shaped enclosure subjected to an oriented magnetic field, ApplThermEng. 168 (2020) 114789, https://doi.org/10.1016/j.applthermaleng.2019.114789.
[19] M. Waqas, Simulation of revised nanofluid model in the stagnation region of cross fluid by expanding-contracting cylinder, Int. J. Numer. Method. Heat. Fluid. Flow 30 (4) (2019) 2193–2205, https://doi.org/10.1108/HFF-12-2018-0797.
[20] A.S. Dogonchi, M. Hashemi-Tilehnoee, M. Waqas, S.M. Seyyedi, I.L. Animasaun, D. D. Ganji, The influence of different shapes of nanoparticle on Cu–H_2O nanofluids in a partially heated irregular wavy enclosure, Phys. A: Statist. Mech. Applic. 540 (2020) 123034, https://doi.org/10.1016/j.physa.2019.123034.
[21] L.A. Lund, A. Wakif, Z. Omar, I. Khan, I.L. Animasaun, Dynamics of water conveying copper and alumina nanomaterials when viscous dissipation and thermal radiation are significant: single-phase model with multiple solutions, Math. Method. Appl. Sci. 46 (10) (2023) 11603–11617, https://doi.org/10.1002/mma.8270.
[22] A. Khan, B. Hassan, E.E. Ashraf, S.Y.A. Shah, Thermally dissipative micropolar hybrid nanofluid flow over a spinning needle influenced by Hall current and gyrotactic microorganisms, Heat Transf. 51 (1) (2022) 1170–1192, https://doi.org/10.1002/htj.22347.
[23] A. Khan, A. Saeed, A. Tassaddiq, T. Gul, P. Kumam, I. Ali, W. Kumam, Bio-convective and chemically reactive hybrid nanofluid flow upon a thin stirring needle with viscous dissipation, Sci. Rep. 11 (1) (2021) 8066, https://doi.org/10.1038/s41598-021-86968-8.
[24] M. Waseem, T. Gul, I. Khan, A. Khan, A. saeed, I. Ali, P. Kumam, Gravity-driven hydromagnetic flow of couple stress hybrid nanofluid with homogenous-heterogeneous reactions, Sci. Rep. 11 (1) (2021) 17498, https://doi.org/10.1038/s41598-021-97045-5.
[25] L.S. Sundar, K.V.V. Chandra Mouli, Z. Said, A.C.M. Sousa, Heat transfer and second law analysis of ethylene glycol-based ternary hybrid nanofluid under laminar flow, J. Therm. Sci. EngAppl. 13 (5) (2021), https://doi.org/10.1115/1.4050228.
[26] R.R. Sahoo, Heat transfer and second law characteristics of radiator with dissimilar shape nanoparticle-based ternary hybrid nanofluid, J. Therm. Anal. Calorim. 146 (2) (2021) 827–839, https://doi.org/10.1007/s10973-020-10039-9.
[27] S. Manjunatha, V. Puneeth, B.J. Gireesha, A.J. Chamkha, Theoretical study of convective heat transfer in ternary nanofluid flowing past a stretching sheet, J. Appl. Comput. Mech. (2021), https://doi.org/10.22055/jacm.2021.37698.3067.
[28] U.S. Mahabaleshwar, K.M. Nihaal, L.M. Pérez, H.F. Oztop, An analysis of heat and mass transfer of ternary nanofluid flow over a Riga plate: newtonian heating, Num. Heat Transf., Part B: Fundam. (2023) 1–16, https://doi.org/10.1080/10407790.2023.2282165.
[29] M. Mumtaz, S. Islam, H. Ullah, Z. Shah, Chemically reactive MHD convective flow and heat transfer performance of ternary hybrid nanofluid past a curved stretching sheet, J. Mol. Liq. 390 (2023) 123179, https://doi.org/10.1016/j.molliq.2023.123179.
[30] A. Shahzad, F. Liaqat, Z. Ellahi, M. Sohail, M. Ayub, M.R. Ali, Thin film flow and heat transfer of Cu-nanofluids with slip and convective boundary condition over a stretching sheet, Sci. Rep. 12 (1) (2022) 14254, https://doi.org/10.1038/s41598-022-18049-3.
[31] W. Ibrahim, O.D. Makinde, The effect of double stratification on boundary-layer flow and heat transfer of nanofluid over a vertical plate, Comput. Fluid. 86 (2013) 433–441, https://doi.org/10.1016/j.compfluid.2013.07.029.
[32] D. Srinivasacharya, M. Upendar, Effect of double stratification on MHD free convection in a micropolar fluid, J. Egypt. Math. Soc. 21 (3) (2013) 370–378, https://doi.org/10.1016/j.joems.2013.02.006.
[33] D. Srinivasacharya, O. Surender, Non-darcy mixed convection in a doubly stratified porous medium with Soret-Dufour effects, Int. J. Eng. Math. 2014 (2014) 1–9, https://doi.org/10.1155/2014/126218.
[34] D. Srinivasacharya, O. Surender, Effect of double stratification on mixed convection boundary layer flow of a nanofluid past a vertical plate in a porous medium, ApplNanosci. 5 (1) (2015) 29–38, https://doi.org/10.1007/s13204-013-0289-7.
[35] P.S. Reddy, P. Sreedevi, Impact of chemical reaction and double stratification on heat and mass transfer characteristics of nanofluid flow over porous stretching sheet with thermal radiation, Int. J. Amb. Energy 43 (1) (2022) 1626–1636, https://doi.org/10.1080/01430750.2020.1712240.
[36] Y.S. Daniel, Z.A. Aziz, Z. Ismail, F. Salah, Double stratification effects on unsteady electrical MHD mixed convection flow of nanofluid with viscous dissipation and Joule heating, J. Appl. Res. Technol. 15 (5) (2017) 464–476, https://doi.org/10.1016/j.jart.2017.05.007.
[37] Y.Q. Song, H. Waqas, K. Al-Khaled, U. Farooq, S. Gouadria, M. Imran, S.U. Khan, M.I. Khan, S. Qayyum, Q.H. Shi, Aspects of thermal diffusivity and melting phenomenon in Carreau nanofluid flow confined by nonlinear stretching cylinder with convective Marangoni boundary constraints, Math. Comput. Simul. 195 (2022) 138–150, https://doi.org/10.1016/j.matcom.2022.01.001.
[38] Y.Q. Song, A. Hamid, T.C. Sun, M.I. Khan, S. Qayyum, R.N. Kumar, B. C. Prasannakumara, S.U. Khan, R. Chinram, Unsteady mixed convection flow of magneto-Williamson nanofluid due to stretched cylinder with significant non-

uniform heat source/sink features, Alexand. Eng. J. 61 (1) (2022) 195–206, https://doi.org/10.1016/j.aej.2021.04.089.
[39] W. Cao, I.L. Animasaun, S.J. Yook, V.A. Oladipupo, X. Ji, Simulation of the dynamics of colloidal mixture of water with various nanoparticles at different levels of partial slip: ternary-hybrid nanofluid, Int. Commun. Heat Mass Transf. 135 (2022) 106069, https://doi.org/10.1016/j.icheatmasstransfer.2022.106069.
[40] X. Ji, Y. Liang, W. Cao, Effect of solid volume concentration on rheological properties of Chengdu Clay Slurry, Processes 10 (2) (2022) 425, https://doi.org/10.3390/pr10020425.
[41] M. Fakour, A. Rahbari, E. Khodabandeh, D.D. Ganji, Nanofluid thin film flow and heat transfer over an unsteady stretching elastic sheet by LSM, J. Mech. Sci. Technol. 32 (1) (2018) 177–183, https://doi.org/10.1007/s12206-017-1219-5.
[42] T. Nagaraju, Tanuja, K. Linganna, S.V. Varma, S. Channaiah, R.S.V. Kumar, U. Khan, T. Muhammad, M.M.M. Abdou, Thermal analysis of natural convection in rectangular porous fin wetted with CNTs nanoparticles and thermal radiation, ZAMM-J. Appl. Math. Mechanics/Zeitschrift. für. Angewandte. Mathematik. und. Mechanik. (2024) e202300969, https://doi.org/10.1002/zamm.202300969.
[43] T.N. Tanuja, K.U. Rehman, G.V. Kumar, W. Shatanawi, S.V.K. Varma, Z. Asghar, On thermal performance of spine fin in magnetized hybrid fluid rooted with Cu and MoS_4 nanoparticles, AIP Adv. 14 (1) (2024), https://doi.org/10.1063/5.0176878.
[44] T.N. Tanuja, et al., Leveraging artificial neural networks approach for thermal conductivity evaluation in porous rectangular wetted fins filled with ternary hybrid nanofluid, J. Radiat. Res. Appl. Sci. 17 (4) (2024) 101125, https://doi.org/10.1016/j.jrras.2024.101125.
[45] H.R. Patel, S.D. Patel, R. Darji, Mathematical Study of unsteady micropolar fluid flow due to non-linear stretched sheet in the presence of magnetic field, Int. J. Thermofluid. 16 (2022) 100232.
[46] M.S. Arif, K. Abodayeh, Y. Nawaz, Design of finite difference method and neural network approach for Casson nanofluid flow: a computational study, Axioms 12 (6) (2023) 527.
[47] A. Raje, A.A. Bhise, A. Kulkarni, Entropy analysis of the MHD Jeffrey fluid flow in an inclined porous pipe with convective boundaries, Int. J. Thermofluid. 17 (2023) 100275.
[48] Y. Nawaz, M. Shoaib Arif, K. Abodayeh, Predictor–corrector scheme for electrical magnetohydrodynamic (MHD) Casson nanofluid flow: a computational study, Appl. Sci. 13 (2) (2023) 1209.
[49] M.S. Arif, K. Abodayeh, Y. Nawaz, Explicit computational analysis of unsteady maxwell nanofluid flow on moving plates with stochastic variations, Int. J. Thermofluid. 23 (2024) 100755.
[50] D. Ali, H. Ullah, A.M. Alqahtani, M. Fiza, A.SA Omer, I. Khan, A.U. Jan, Numerical treatment of squeezed fluid flow under the magnetic influence amid parallel disks, Int. J. Thermofluid. (2024) 100723.
[51] R. Manaswini, B.N. Hanumagowda, T.N. Tanuja, L. Kavitha, A. Abdulrahman, R. J. Punith Gowda, S.V.K. Varma, Sensitive analysis of heat transfer enhancement in ternary Casson nanofluid flow between a conical surface and disk, Mod. Phys. Lett. B (2024), https://doi.org/10.1142/S0217984924504207.
[52] H. Hanif, W. Jamshed, M.R. Eid, R.W. Ibrahim, S. Shafie, A.A. Raezah, S.M. El Din, Numerical Crank-Nicolson methodology analysis for hybridity aluminium alloy nanofluid flowing based-water via stretchable horizontal plate with thermal resistive effect, Case Stud. Therm. Eng. 42 (2023) 102707.
[53] M. Yasir, M. Khan, A.S. Alqahtani, M.Y. Malik, Heat generation/absorption effects in thermally radiative mixed convective flow of Zn− TiO2/H2O hybrid nanofluid, Case Stud. Therm. Eng. 45 (2023) 103000.
[54] Y.-Q. Song, B.D. Obideyi, N.A. Shah, I.L. Animasaun, Y.M. Mahrous, J.D. Chung, Significance of haphazard motion and thermal migration of alumina and copper nanoparticles across the dynamics of water and ethylene glycol on a convectively heated surface, Case Stud. Therm. Eng. 26 (2021) 101050.